A 3D hp-Discontinuous Galerkin Method: Revisiting the M7.3 Landers Earthquake

J. Tago[1], V.M. Cruz-Atienza[1], J. Virieux[2], V. Etienne[3] and F.J. Sánchez-Sesma[4]

(1) Instituto de Geofísica, UNAM, Mexico (josue.tago@gmail.com); (2) Institut des Sciences de la Terre, UJF, Grenoble, France; (3) Géoazur, UNSA- CNRS, Nice, France; (4) Instituto de Ingeniería, UNAM, Mexico.

AGU FALL MEETING 2011
S43C-2263

1. Introduction

Considering the dynamics of the rupture process is fundamental for simulating ***realistic seismic scenarios*** useful for seismic hazard mitigation**.** We chose to extend the *hp-adaptive 3D Discontinuous Galerkin Finite Element* code (DG-FEM)[1] to integrate the fault dynamics.

The dynamic rupture formulation requires ***explicit boundary conditions*** over the surface describing the fracture. These boundary conditions are treated such that physical conditions previously estimated are respected. This implies special treatment for the fault fluxes where discontinuities of the velocity field are allowed.

The fault strength follows a *linear slip-weakening law*, although any other ***friction law*** could be implemented. Besides, an *artificial viscous damping* has been applied to reduce spurious numerical oscillations.

We have solved two ***SCEC benchmarks*** [4] to verify our formulation with the state of the art. We are currently modeling the ***1992 Landers earthquake***, for which both the fault system geometry and the velocity structure play a critical rol in rupture dynamics.

2. Discontinuous Galerkin-Finite Element Method

Our DG-FEM numerical method combines features of the Finite Element and the Finite Volume frameworks. The method works with the weak formulation of the ***elastic first order hyperbolic velocity-stress system*** of equations in a discrete domain described by a non-structured tetrahedral mesh. Since the scheme doesn't require to verify continuity between adjacent elements, it's very suitable for treating non-linear discontinuous phenomena, like the dynamic rupture.

The code has several main features:

1) The **Convolutional Perfectly Matched Layers** (CPML) absorbing boundary conditions to simulate an unbounded medium without spurious reflections.

2) The **h-adaptivity** that allows refining the mesh according to the physical properties and geometry of the model. This enhances the accuracy of the scheme and minimize the computational load. Furthermore this allows controlling the number of elements within the absorbing CPML (Figure 1) independently of the physical domain.

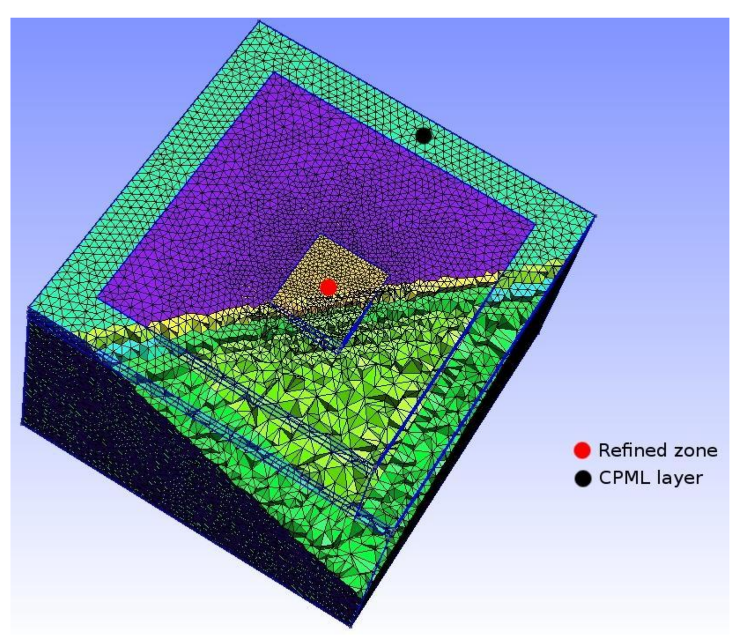

Figure (1) Example of an unstructured mesh

3) The **p-adaptivity** that allows choosing the order of the approximation in every tetrahedron of the mesh (Figure 2), e.g. elements with P0 approximation within the CPML and elements with both P1 and P2 approximations depending on their sizes within the physical domain.

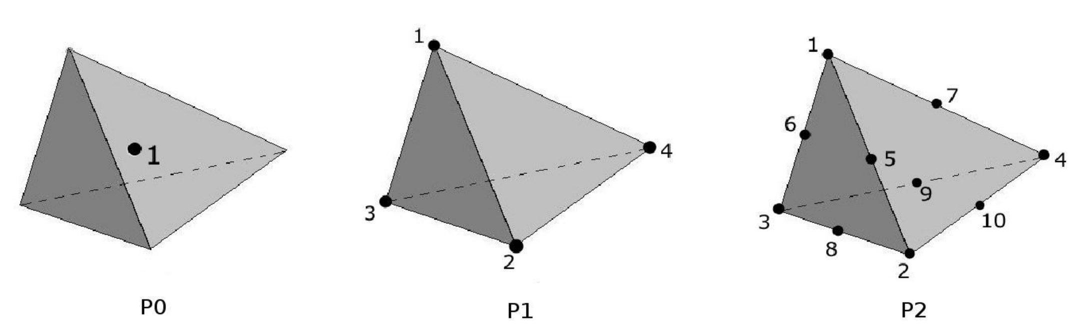

Figure (2) Degrees of freedom for the different approximation orders we use.

4) A **parallel implementation** for supercomputing using the Message Passing Interface (MPI) library.

3. Dynamic rupture

The mathematical and computational modeling of the dynamic rupture was made following a previously work [2] based on a 3D finite volume approach (i.e. P0 approximation). In our ongoing study we use P2 elements over the fault and use the p-adaptivity everywhere else (P0, P1 or P2 approximations).

3.1 Crack boundary conditions

Over the crack surface Γ the friction coefficient μ is assumed to follow a ***linear slip-weakening law*** so that the frictional strength τ_c evolves as

$$\tau_c = -\sigma_N \mu \qquad (1)$$

where σ_N is the fault normal stress. Besides, the frictional strength τ_c, the slip rate $\underline{V}$ and the tangential traction $\underline{T}_T$ over the fault must follow the jump conditions

$$\tau_c - \|\underline{T}_T\| \geq 0 \qquad (2.1)$$

$$\tau_c \underline{V} - \underline{T}_T \|\underline{V}\| = 0 \qquad (2.2)$$

which prevent retrograde fault motion and allow rupture healing.

To compute the tangential fault traction, $\underline{T}_T$, we implemented a ***predictor-corrector scheme*** to guarantee that every fault node respect eq. 2.1 at any time. Simultaneously, the normal fault traction, $\underline{T}_N$, is computed in such a way that ***continuity of the normal velocity*** across the fault is verified.

To diminish numerical oscilations we apply an ***artificial viscous damping.*** The damping is controled by the parameter η involved in the equation of motion only over the fault nodes as proposed in [3] .

4. Model verification

4.1 TPV3 SCEC Benchmark

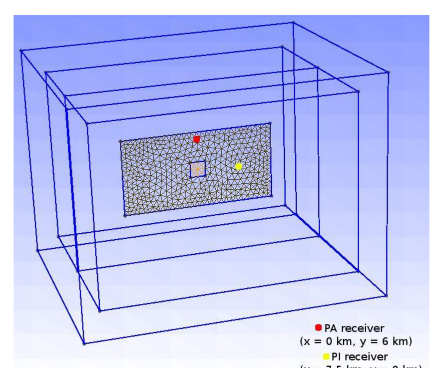

Figure (3) TPV3 fault geometry and receivers (color dots). Simulation box in blue lines.

TPV3 is a SCEC benchmark [4] considering a ***vertical strike-slip fault*** embedded in a homogeneous full-space. The initial shear and normal fault tractions are constant.

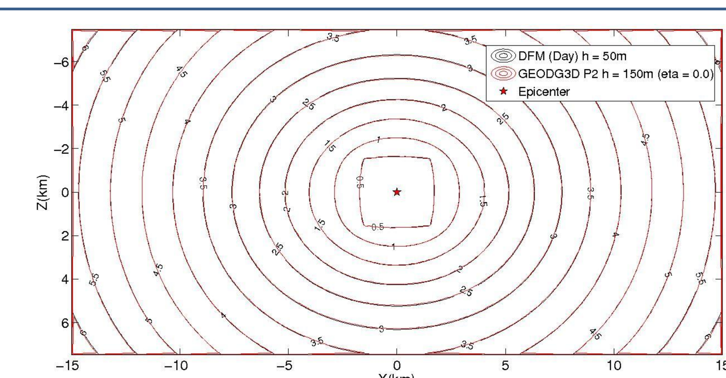

Figure (4) Contour plot for rupture times

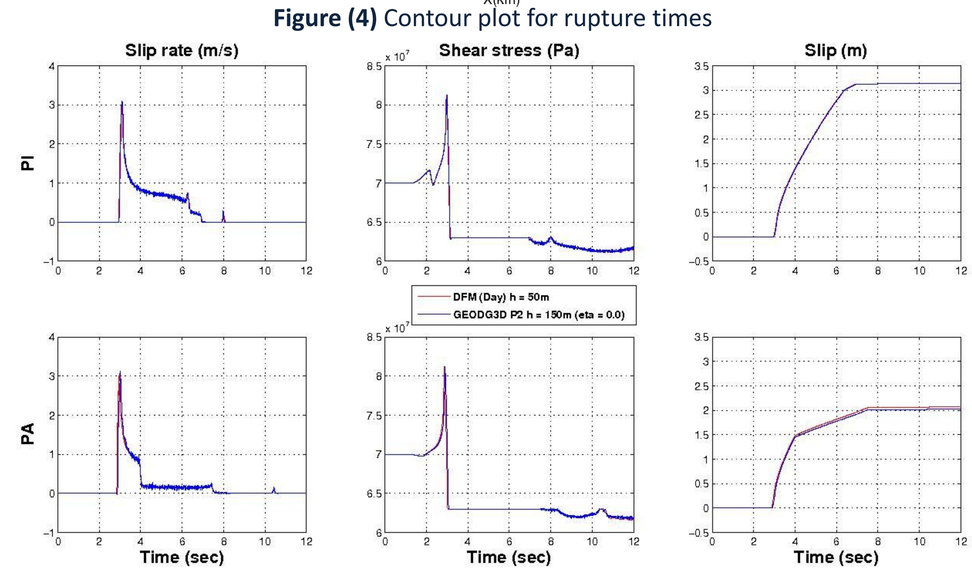

Figure (5) Time histories at both fault receivers PI and PA compared with the DFM finite difference (red) reference solution (Day et al., 2005).

4.2 TPV10 SCEC Benchmark

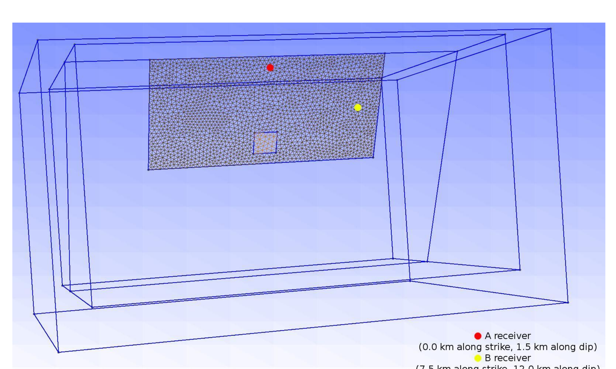

Figure (6) TPV10 fault geometry and receivers (color dots). Simulation box in blue lines.

TPV10 is a SCEC benchmark [4] for a ***60-degree dipping normal fault*** embedded in a homogeneous half-space reaching the free surface. The shear and normal fault tractions are down-dip distance dependent.

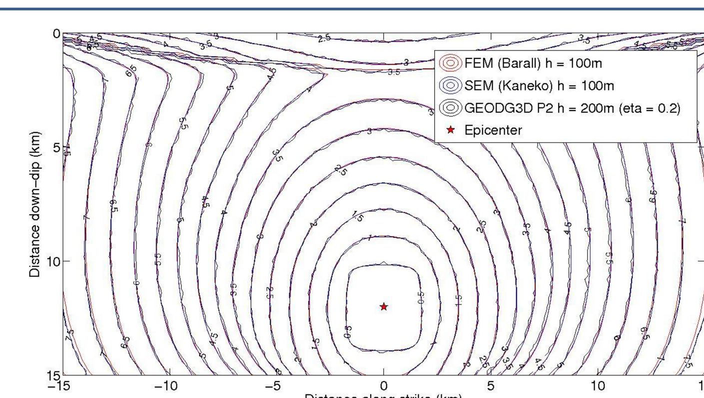

Figure (7) Contour plot for rupture times

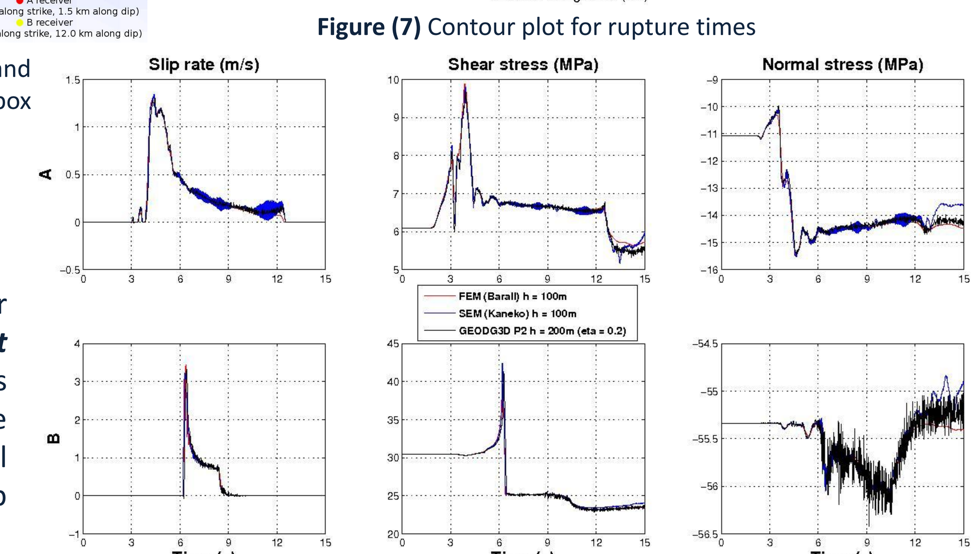

Figure (8) Time histories at both fault receivers compared with finite element (red) and spectral element (blue) solutions by different authors.

5. 1992 Landers Earthquake simulation

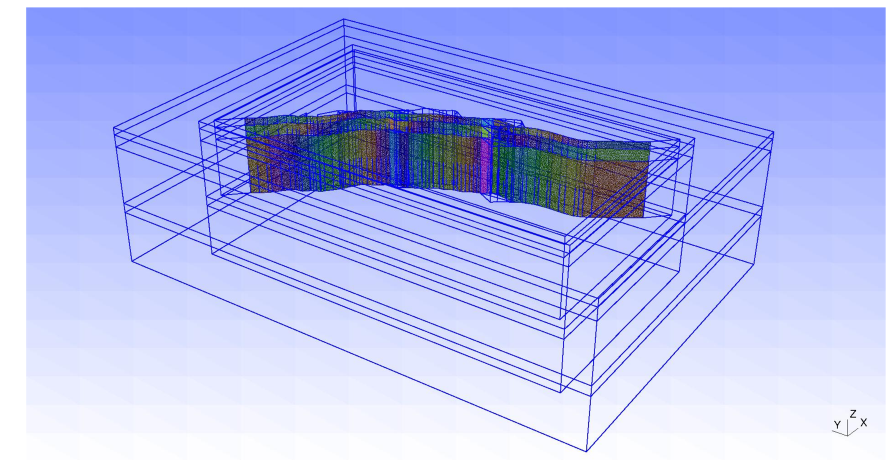

Figure (9) Landers geometry (SCEC Community Fault Model)

For our dynamic rupture simulation of the Landers earthquake we imposed, in our nonplanar fault system geometry (see Figure 9 and Table 1), the ***heterogeneous initial stress*** determined by Peyrat et al. [5] using a planar fault model and the final slip distribution computed by Wald & Heaton [7].

By setting both the Peyrat's prestress and friction parameters, rupture didn't propagate. Only after a strongly reduction of fracture energy, i.e. by ***decreasing the slip weakening distance*** δ_c from 0.8 m to 0.4 m, rupture was allowed to propagate spontaneously.

The ***final slip distribution*** should be similar to Wald & Heaton's slip. However, due to high stress drop close to the free surface the slip was considerably overpredicted. To avoid this, we applied a 2 km length superficial taper to the initial shear stress and reduced 5% the maximum shear stress in the whole fault. A comparison of the final slip distribution and rupture times, can be seen in Figures (12) and (13) and snapshots of the slip rate and shear stress in Figures (10) and (11), respectively.

From the final slip distribution is clear that the geometry plays a major role in Landers earthquake dynamics. Besides recomputing the initial fault tractions in the real fault geometry, we will also explore the ***friction parameters*** as observed by Aochi et al.[8].

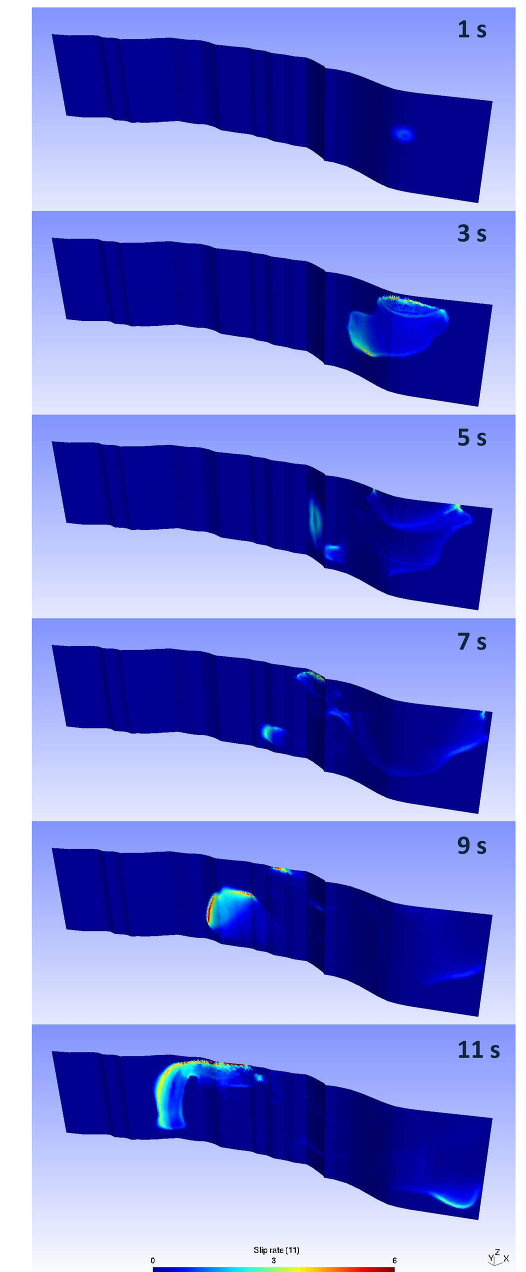

Figure (10) Snapshots of the slip rate

Rupture front jump

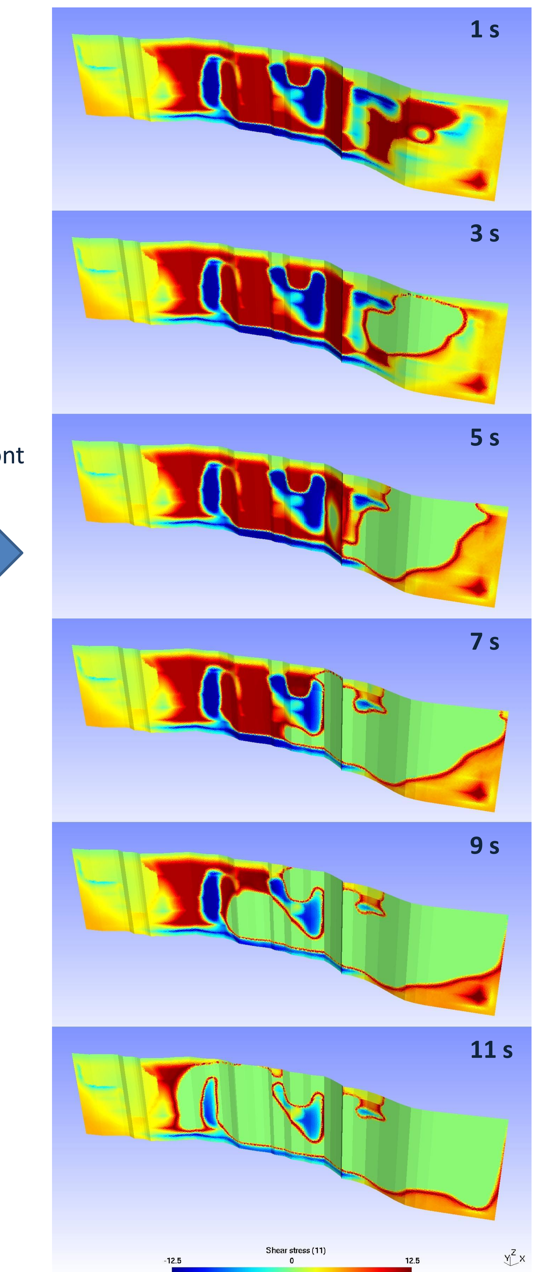

Figure (11) Snapshots of the shear stress

Vp (km/s)	Vs (km/s)	Density (g/cm³)	Thickness (km)
3.80	1.98	2.30	1.5
5.50	3.15	2.60	2.5
6.20	3.52	2.70	22.0

Table (1) Regional velocity structure from [7]

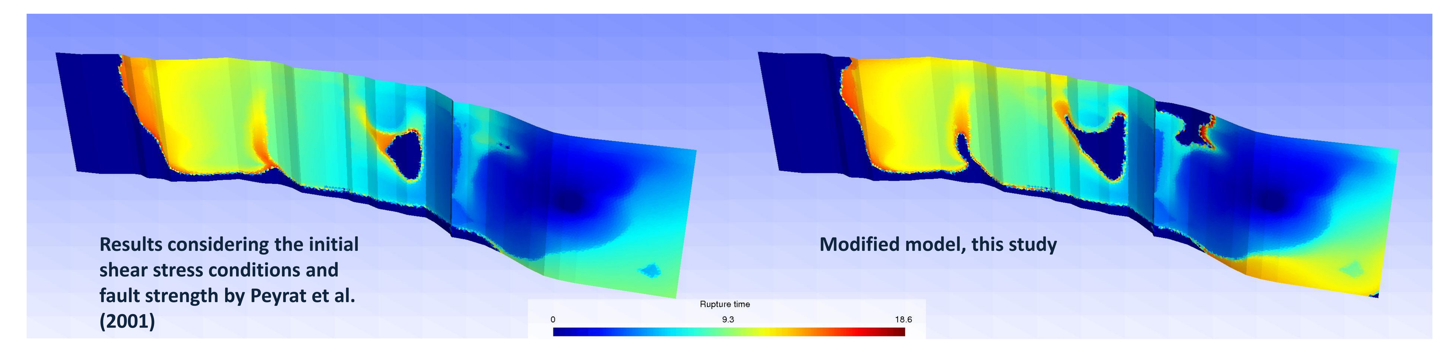

Figure (12) Rupture time

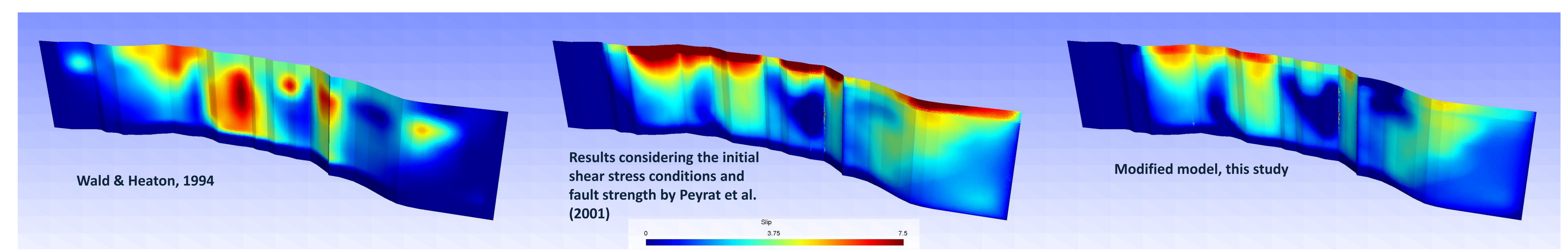

Figure (13) Final slip

6. Conclusions

We have succesfully implemented a dynamic rupture model in our hp-Galerkin Discontinuous scheme. We've been able to overcome the lack of convergence from our previous implementation, using only P0 elements in the fault, of Benjemaa's work by developing new strategies which allow using ***P2 fault elements***.

Before applying our computational model to the Landers earthquake, we first verified it throughout ***SCEC benchmarks***. Solving the TV10 benchmark was critical because it assumes a heterogeneous initial *stress in a dipping normal fault reaching the free surface, which requires a accurate solution of dynamic normal stresses over the fault.*

Our simulations of the Landers earthquake show that **fault geometry is critical** to estimate a realistic initial fault-traction condition and avoiding unrealistically high stress concentrations. We will shortly recompute the initial stress field to explain the available seismograms and study the fault friction parameters following [8].

7. References

[1] Etienne V., E. Chaljub, J. Virieux and N. Glinsky, "An hp-adaptive discontinuous Galerkin finite-element method for 3-D elastic wave propagation", Geophysical Journal International, Vol. 183, 2010.
[2] Benjemaa M., N. Glinsky, V.M. Cruz-Atienza and J. Virieux, "3-D dynamic rupture simulations by a finite volume method", Geophysical Journal International, Vol. 178, 2009.
[3] Dalguer Luis A. and Steven M. Day, "Staggered-grid split-node method for spontaneous rupture simulation", Journal of Geophysical Research, Vol. 112, 2007.
[4] Harris R.A. et al., " The SCEC/USGS Dynamic Earthquake Rupture Code Validation Exercise", Seismological Research Letters, Vol. 80, 2009.
[5] Peyrat Sophie, Kim Olsen and Raúl Madariaga, "Dynamic modeling of the 1992 Landers earthquake", Journal of Geophysical Research, Vol. 106, 2001.
[6] Geuzaine C. and J.-F. Remacle, "Gmsh: a three-dimensional finite element mesh generator with built-in pre- and post-processing facilities", International Journal for Numerical Methods in Engineering, Vol. 79, 2009.
[7] Wald, D. and T. Heaton, "Spatial and temporal distribution of slip for the 1992 Landers, California, earthquake", Bull. Seismol. Soc. Am., Vol. 84, 1994.
[8] Aochi, H., R. Madariaga, and E. Fukuyama, "Constraint of fault parameters inferred from nonplanar fault modeling", Geochem. Geophys. Geosyst, Vol. 4, 2003.